Robust Control Strategies on the Optimization of a Wind Turbine Pumping System

Olfa Gam *, Riadh Abdelati *‡, Mahamadou Abdou Tankari **,

Mohamed Faouzi Mimouni*, Gilles Lefebvre**

* Department of Electrical Engineering, Unit ESIER, National School of Engineers of Monastir, University of Monastir, Tunisia

** CERTES Laboratory, Paris Est Crteil, 61, Avenue du Gnral De Gaulle, 94010, Creteil Cedex

(phdolfa2015@gmail.com, riaabdelati@yahoo.fr, mahamadou.abdou-tankari@u-pec.fr)

‡ Corresponding Author; Second Author, University of Monastir, Av. Ibn El Jazzar Skanes (5019), Tunisia,

Tel: +216 55 854232,

Received: 30.04.2018 Accepted:04.07.2018

Abstract- Wind Turbine water pumping system (WTWPS) has been an important area of research during these last years. The control of WTWPS has attracted researchers from different fields to improve the effectiveness of water pumping systems. In this paper, we focus on the study of a pumping system composed by a wind turbine, permanent magnet synchronous generator, an induction motor (IM), and a centrifugal pump. Our purpose is to keep the water pumping in optimum conditions and maximize the extracted wind power. In a first step, we analyze the operation of WTWPS at variable speed with pitch angle control to ensure the required power without mechanical failure. The principle source and the dynamic load were connected via a direct current bus. On the other hand, to achieve the feeding of the moto-pump with a good quality of electrical energy, an analytic equation is developed which adapts the set point rotation speed of induction machine regardless the state of wind velocity. A nonlinear DTC control strategy is adopted based on space vector pulse width modulation. Simulation results are performed in MATLAB environment and show the performance and capability of the proposed control scheme of WTWPS. .

Keywords Wind energy, Optimization, Water pumping, Direct torque control, Energy optimization.

1. Introduction

In the last decades, the necessity of optimizing of water exploitation and energy resources has become an essential issue and it will be more vital in the future [1]. Due to the exhaustion increase of human consumption, the limited reserves on conventional energy resources such as natural gas, coal and oil) and the degradation of environmental conditions, renewable sources (such as biomass, solar photovoltaic, wind and hybrid forms of energy) have become an alternative solution to reduce the dependence on fossil fuels to generate electricity [2]. For instance, in a remote agricultural area, the demand of electrical energy supply systems is increasing for desalination, water pumping and supplying isolated dwellings with electricity. Among all renewable energy resources, the wind energy is considered as the most promising generator thanks to its availability in most remote areas [3]. Moreover, pumping water presented one of the applications that mostly needs the use of wind turbines. Because, when a wind turbine is powering a water pumping system, it can easily establish a natural relationship between water requirement and the wind power availability [4]. WTWPS are particularly suitable with their different mechanical, electrical and electronic components for water pumping. Several types of WT are used for isolated regions. Previous studies indicated that variable speed turbines are much more efficient in energy capture compared with constant speed turbine [5]. Several control strategies are developed by researchers in order to improve and make WTWPS more efficient and reliable. Many other works, focus on new techniques to improve the output controllability of wind energy systems. In this context, several methods have been proposed to extract a maximum power from wind turbines, using fuzzy logic, perturb and observer (P and O) technique and neural networks [6]. However, most of the previous studies have not taken into account the interaction between power delivered by the source, the environmental conditions and the pumping power.

This paper presents a novel method to achieve an optimal operation of water pumping system using an IM powered by a wind turbine. Moreover, the proposed method develops a robust control algorithm which aims to maximize the output power of a variable speed wind turbine (VSWT) and at the same time, guarantees an optimum power for water pumping. As wind source variation affects the technical system feasibility. This has been taken into consideration to establish a complete mathematical model. Our proposed algorithm offers a nonlinear control of the IM motor for different operating points. This strategy can offer a maximum energy for water pumping.

The paper is organized as follows: Starting with an introduction in Section 2, Section 2 describes the wind turbine water pumping system and section 3 develops the model of the pumping unit. The proposed control strategies is presented in section 4. Finally, in section 5, the strategy is applied to the WTWPS system and evaluated for different environment conditions. The conclusions are presented at the end of the paper.

2. Wind Turbine Water Pumping System Description

The WTWPS scheme structure used in our study is illustrated by Fig.1. It consists of the electric generating unit, a pumping unit and a tank used as a water storage device.

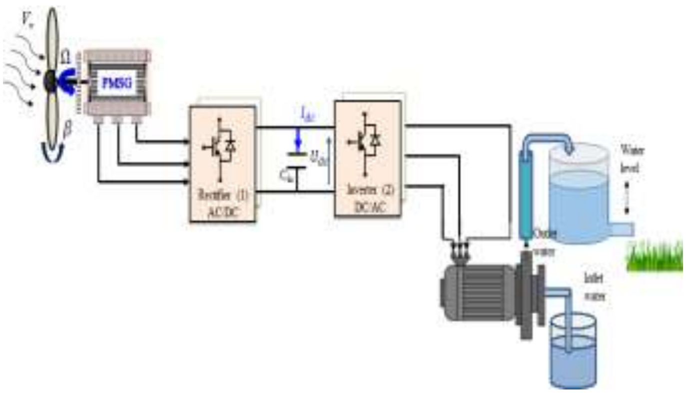

Fig. 1. The WTWPS scheme structure

2.1. Mathematical modeling of wind turbine generator

The output power extracted from WT system is described as follows [7,8]:

$$P_{WT} = \frac{1}{2}\rho S C_p(\lambda,\beta) V_w^3 \quad (1)$$

Where ρ is the air specific density (typically 1.225 kg/m3), S is the area swept by the C_p is the coefficient of power conversion and V_w is the wind velocity in (m/s).

P_{WT} is determined by the power coefficient of the wind turbine system. The generic equation used to model the power coefficient $C_p(\lambda,\beta)$ based on the turbine model characteristics and described in [9] is given by Eq. (2) :

$$C_p(\lambda,\beta) = 0.53\left[\frac{151}{\lambda_i} - 0.58\beta - 0.002\beta^{2.14} - 13.2\right] exp(\frac{-18.4}{\lambda_i}) \quad (2)$$

Where
$$\lambda_i = \frac{1}{\frac{1}{\lambda - 0.02\beta} - \frac{0.003}{\beta^3+1}} \quad (3)$$

Where λ is the tip speed ratio of the tangential velocity given by the equation (4):

$$\lambda = \frac{R_t \Omega_t}{V_w} \quad (4)$$

With Ωt and R_t are the rotor angular velocity in (rad/s) and rotor radius in (m) respectively. $C_p(\lambda,\beta)$ versus λ are illustrated in Fig. 2 for different pitch angle β values

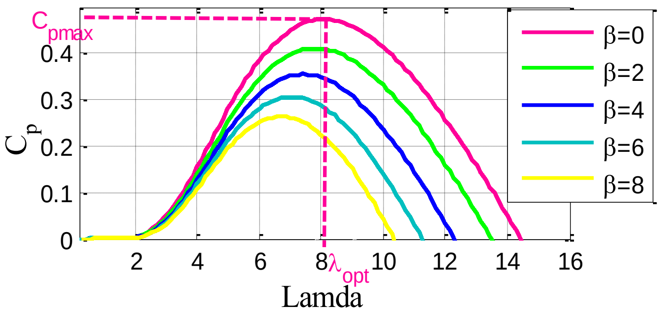

Fig. 2. Cp curves for different values of β.

2.2. *Pitch controller*

For high speed, the pitch control of the blades is an essential method to protect the electrical and mechanical components. Figure 3 shows the block diagram of the pitch angle control system using a proportional integral (PI). Taking into consideration the blade's orientation system, the transfer function of the pitch angle control can be given by:

$$\beta = \frac{1}{1+\tau_b S}\beta_{ref} \quad (5)$$

With τ_b is the response time.

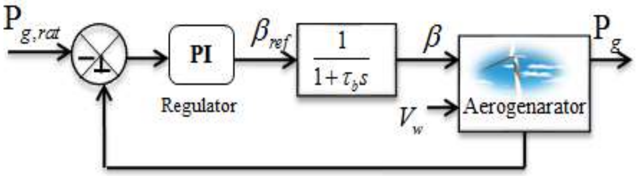

Fig. 3. Pitch angle control strategy

2.3. Modeling and vector control strategy of PMSG

The considered PMSG is a permanent magnet machine with radial magnetization. By applying the park reference frame, PMSG model is expressed by [7]:

$$\begin{pmatrix} V_{gd} \\ V_{gq} \end{pmatrix} = -R_s \begin{pmatrix} I_{gd} \\ I_{gq} \end{pmatrix} - \frac{d}{dt}\begin{pmatrix} L_d I_{gd} \\ L_q I_{gq} \end{pmatrix} + p\Omega_t \begin{pmatrix} 0 & 1 \\ 1 & 0 \end{pmatrix} \begin{pmatrix} L_d I_{gd} + \phi_m \\ L_q I_{gq} \end{pmatrix} \quad (6)$$

The WT and PMSG parameters are given in Table 1 where Rs is the stator winding resistance (Ω), $L_d = L_q = L_s$: are the stator winding inductance (H), Φ_m is the permanent rotor flux (wb), V_{gd} and V_{gq} are the d-q components of the stator voltages (V) respectively, w is the rotational speed (rad s-1) and p is the number of pole pairs.

Table 1. WT and PMSG parameters.

Symbol	**Value**	**Symbole**	**Value**
R_t	2 m	P	4
λ_{opt}	8.1	Rs	0.82 Ω
C_{pmax}	0.472	Ld=Lq	15.1 mH
P_N	3.9 kw	ϕm	0.5 wb

Thus, the electromagnetic torque can be expressed by [10]:

$$T_{emg} = p\phi_m \phi I_{sq} \quad (7)$$

Two conventional and proportional integrator are proposed to the control loop of direct and quadrature currents respectively Isd and Isq as shown in Fig. 4:

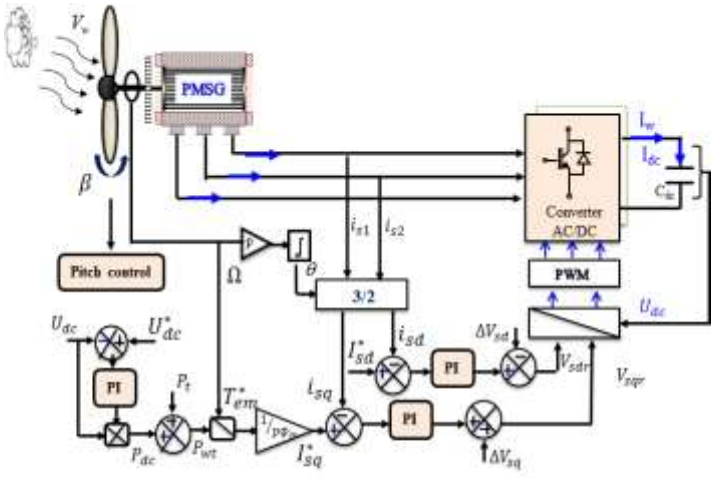

Where $\Delta V \Delta V_{sq} = \omega_e \Phi_m + L\omega_e I_{sd}$, $\Delta V_{sd} = L\omega_e I_{sq}$, $\omega_e = p\Omega_t$ denoted by compensating voltages

Fig.4. Synoptic of the control strategy applied to WT based on PMSG

3. Water Pump-induction Motor: Mathematical Model

3.1. Mathematical model of water pump IM

The pumping unit used in our simulation has a 3 Kw asynchronous motor with 2 poles pairs (Np = 2). The IM is mechanically coupled to a centrifugal pump of same equivalent power. The equivalent model of the symmetrical IM, can be represented in the reference rotating frame (d-q) by considering the flux orientation Φr on the d-axis as:

$$\begin{cases} \dfrac{dI_{sd}}{dt} = -\gamma I_{sd} + w_s I_{sq} + K\alpha_r \phi_{rd} + K w_r \phi_{rq} + \dfrac{1}{\sigma L_s} U_{sd} \\ \dfrac{dI_{sq}}{dt} = -w_s I_{sd} - \gamma I_{sq} - K w_r \phi_{rd} + K\alpha_r \phi_{rq} + \dfrac{1}{\sigma L_s} U_{sq} \\ \dfrac{d\phi_{rd}}{dt} = M\alpha_r I_{sd} - \alpha_r \phi_{rd} + w_{sl}\phi_{rq} \\ \dfrac{d\phi_{rq}}{dt} = M\alpha_r I_{sq} - w_{sl}\phi_{rd} - \alpha_r \phi_{rq} \\ \dfrac{dw_r}{dt} = \dfrac{np}{j}(T_e - T_L) - \dfrac{f}{j} w_r \end{cases} \quad (8)$$

where Isd; Isq : stator current, Φ_{rd}; Φ_{rq}: rotor fluxes and the electrical rotor speed wr are the state variables. Both the stator voltages U_{sd}; U_{sq} and the slip frequency ws are considered as the control variables. With the constants defined as:

$$R_\lambda = R_s + \frac{M^2}{L_r^2} R_r, \sigma = 1 - \frac{M^2}{L_r L_s}, \mu = \frac{M}{L_r}, k = \frac{1}{\sigma L_s}\mu, \gamma = \frac{1}{\sigma L_s} R_\lambda, \alpha_r = \frac{1}{Tr}$$

The electromagnetic torque expressed in terms of the state variables is given by:

$$T_e = \frac{3}{2}\frac{n_p M}{L_r}(\phi_{rd} I_{sq} - \phi_{rq} I_{sd}) \qquad (9)$$

Parameters of the induction motor are listed in Table 2.

Model Parameter			
Pn: Output power	3 Kw	L_r :Rotor inductance	0.1164 H
Vs :Stator voltage	220 V	l_s :Stator leakage inductance	0.024 H
N_p : Pole number	2	l_r :Rotor leakage inductance	0.024 H
R_s :Stator resistance	1.411 Ω	M_{sr} :Mutual inductance	0.1113 H
R_r: Rotor resistance	1.045 Ω	J : Inertia moment	0.116 kgm2
L_s :Stator inductance	0.1164 H	f : friction coefficient	6.46 e^{-3} Nms

Table 2. Induction machine parameters and its nominal values.

3.2. Water pump

The centrifugal pumps are commonly used since they require less torque to start and produce more head than other dynamic pumps at variable speed operation [11].
For those reasons, we opt for the centrifugal pump. Its load torque is proportional to the square of the rotor speed:

$$T_L = K_L \Omega^2 \qquad (10)$$

Where $K_L = \frac{T_{e-max}}{\Omega_{max}}$: the constant characteristic of the pump. T_{e-max}: the maximum torque and Ωmax: the maximum speed. To determine the performance (Q'; H'; and P') for a speed N', we use the laws of similarity with known performance of the centrifugal pump (Q; H; and P) given by the following relationships [12]:

$$Q' = Q\frac{N'}{N},\ H' = H\left(\frac{N'}{N}\right)^2,\ P' = P\left(\frac{N'}{N}\right)^3$$

where Q and Q' correspond to the flow speed N and N' respectively, H and H' are the total discharge heads, and P and P' are the powers of the IM also corresponding to the speed N and N' respectively [13]. With a flow rate Qe from the top, the water enters and exits a tank through a valve hung in its base. A differential equation of the liquid height in the tank is given by:

$$V^{\cdot} = Sh^{\cdot} = Q_e - Q_s \qquad (11)$$

Where V is the liquid volume in the tank, S is the cross sectional area of the tank, h is the height of the liquid.

4. Control Strategy

Our goal is to maximize the volume of the water pumped according to the relation between wind power of the WT and the IM's rotor speed. Therefore, we should adopt to the motor-pump instantaneously the maximum of power delivered by the wind energy.

4.1. Optimum set point speed operating by WT

The speed control of the IM and the centrifugal pump driving process are related to the wind velocity V_w according to the mechanical power equation. In optimal operating regime, we can develop a relationship between the extracted power Pa and the one transmitted to the rotor P_t which satisfy the equation (12):

$$P_a - \frac{3}{2}R_s I_s = P_t \qquad (12)$$

Where P_t is described by the equation (13):

$$P_t = T_e \Omega_s = T_e \frac{\omega_s}{N_p} \tag{13}$$

With

$$T_e = K_L \Omega^2 = K_L \frac{\omega^2}{n_p} \tag{14}$$

and Ω_s is the synchronous speed. By introducing the slip frequency and using equation (13) ; P_t can be given by:

$$P_t = \frac{K_L}{N_p^3}(\omega_g + \omega)\omega^2 \tag{15}$$

In addition, the stator current modules is expressed as:

$$I_s = \sqrt{I_{sd}^2 + I_{sq}^2}$$

Therefore, we prove that the slip frequency is estimated based on the quadrature stator current Isq. It is expressed by the following expression:

$$\omega_g = \frac{M_{sr}}{\tau_r}\frac{1}{\phi_r} I_{sq} \tag{16}$$

Referring to equations (14) and (16), the quadrature stator current is expressed as:

$$I_{sq} = \frac{2}{3}\frac{L_r K_L}{n_p^3 M \phi_r}\omega^2 \tag{17}$$

On the other hand, the following Eq. (18) gives the direct component of the stator current:

$$I_{sd} = \frac{\phi_r}{M_{sr}} \tag{18}$$

Replacing I_{sq} with its expression, the slip pulsation becomes:

$$\omega_g = \frac{2}{3}\frac{R_r K_L}{n_p^3 \phi_r^2}\omega^2$$

Inserting the expression of Isd, Is and w_g we obtain:

$$P_a - \frac{3}{2} R_s \left[\left(\frac{\phi_r}{M_{sr}}\right)^2 + \frac{4}{9}\left(\frac{L_r K_L}{n_p^3 M_{sr} \phi_r}\right)^2 \omega^4 \right] = \frac{2}{3} R_r \left(\frac{K_L}{n_p^3 \phi_r}\right)^2 + \frac{K_L}{n_p^3}\omega^3 \tag{19}$$

Where $P_a = P_{WT}$ for each value of V_w.
Finally, the Eq. (20) yields a fourth-order polynomial function versus the rotor speed given by:

$$p(\omega) = a\omega^4 + b\omega^3 + c = 0 \tag{20}$$

With

$$a = \frac{2}{3}\left[\frac{K_L}{N_p^3 \phi_r}\right]^2 \left[R_r + R_s\left(\frac{L_r}{M_{sr}}\right)^2\right], b = \frac{K_L}{n_p^3}, c = \frac{3}{2} R_s \left(\frac{\phi_r}{M_{sr}}\right)^2 - P_{WT}$$

Roots given from Eq. (21) give us an idea about the speed reference level or profiles according to the wind speed values. Those solution are considered as different set-points speed reference at the input controller. These roots give for each wind speed value a corresponding speed value for the machine. Using the fitting technique, we obtain, finally an analytic solution given the reference speed Ωref versus the wind speed. This solution is expressed below:

$$\Omega_{ref} = p_1 V_w^4 + p_2 V_w^3 + p_3 V_w^2 + p_4 V_w + p_5 \tag{21}$$

Figure.5 shows that when the wind speed increases automatically the speed of the machine increases and vice verse.

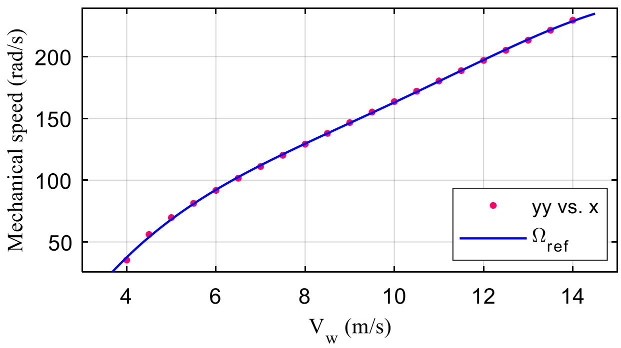

Where $yy = \Omega_{ref}$ and $x = V_\omega$

Fig. 5. Curve of the mechanical speed versus V_w

Coefficients	P1	P2	P3	P4	P5
Value	-0.02255	0.9116	-13.62	105.9	-220.8

Table 3. Different parameters of the analytic solution.

4.2. DTC-SVM Based on the Proportional-Integral-Controllers:

DTC-SVM strategy is considered as one of the variable structure control techniques, which can overcome and eliminate the complexity of moto-pump system [14]. Our

proposed DTC-SVM control scheme is resumed by a pair of conventional PI using in torque and flux controller and an AW-PI speed controller. SVM technique refers to a special switching scheme of six switching cells of a three phase PWM inverter giving eight switching configurations to control the stator flux and eight possible switching combinations to approximate the circle flux reference [15].
For any modulation period T_{mod} of the inverter, SVM technique is provides the suitable inverter's command signal$\vec{V_s}^*$. The selected sector is determined by using the components of the voltage vector ($V_{s\alpha}$; $V_{s\beta}$) as follows:

$$\theta = arctg\left(\frac{V_{s\beta}}{V_{s\alpha}}\right)$$

It can be expressed by:

$$\vec{V_s}^* = V_{s\alpha} + jV_{s\beta} \qquad (22)$$

The structure of the predictive DTC-SVM of the Moto-pump is shown in Fig.6. Then this compound takes the form given by equation (23). The proposed stator flux controller delivers the direct component of the voltage reference.
Then this compound takes the form given by equation (23):

$$V_{sdref} = \Delta\Phi_s\left(K_p + \frac{K_i}{s}\right) \qquad (23)$$

On the other hand, the torque controller offers the quadrature component of V_{sref}.
The equation of V_{sqref} can be written by the following form:

$$V_{sqref} = \Delta T_e\left(K_p + \frac{K_i}{s}\right) + \Phi_S\omega_S \qquad (24)$$

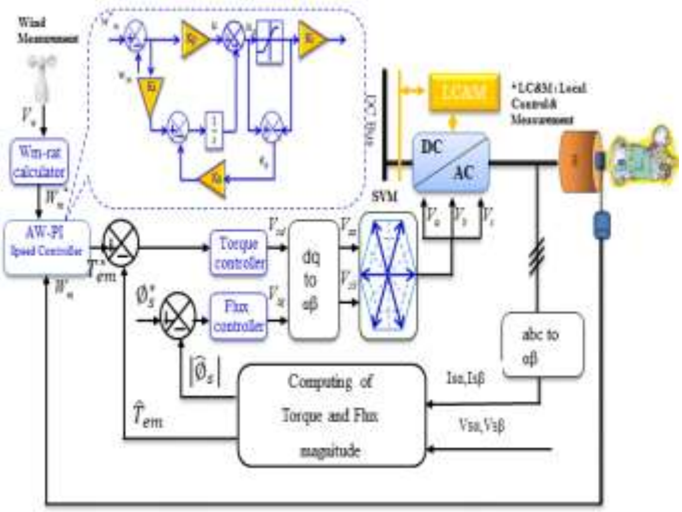

Fig. 6. Scheme of the proposed DTC-SVM

where ω_S is the stator speed. In stator flux reference, the SVM unit receives d - q axis vectors and stator flux position as inputs and it commands in turn the inverter voltage. From the equation (20), the wind speed variation leads to a high set-point change in the mechanical speed of the moto-pump. For this reason, in this context we introduce an anti-windup controller that provides the necessary dynamic to assure the suitable closed loop performance of the moto-pump system. Figure. 6 shows the strategy block diagram used to prevent the integral windup phenomenon caused by the saturation in the PI controller.

5. Results and Discussion

The results of the proposed control strategies for the WTWPS previously described, are presented in this section. The simulation was carried out using the Matlab/Simulink environment, from which the important features of the wind power water pumping systems were evaluated. Under a real wind profile, Fig. 7 (a) to 7(d) show the action of the pitch control to limit the wind power, the WT torque and the power supplied by the wind.

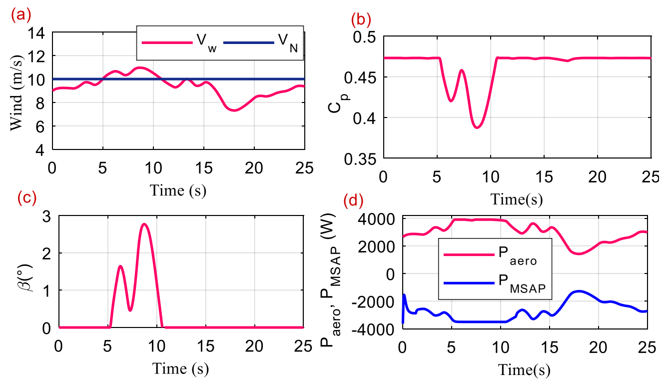

Fig.7. WT set curves for real wind profile a) wind speed profil, b) Power coefficient, c) Pitch angle, d) WT power and PMSG power generated

The electromagnetic torque and quadratic current registered the same behaviour as their references as shown in Fig. 8.

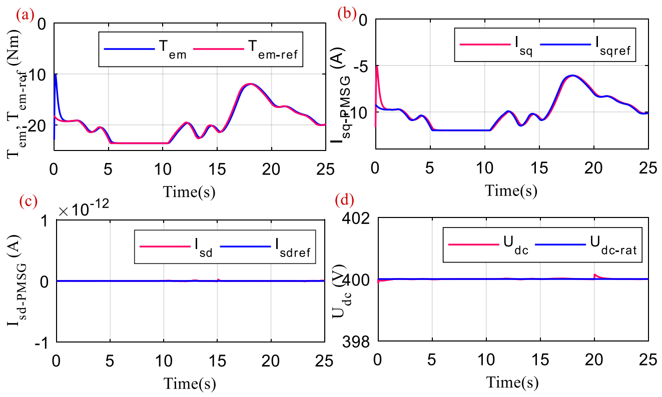

Fig. 8. a) Electromagnetic torque, b) Generated current I_{sq}, c) Generated current I_{sd}, d) DC bus voltage

Figure. 9 shows variables of the pumping unit, the moto-pump speed evolution, the electromagnetic and the load torque, the pump power and the evolution of the water flow. We can observe that the volume of water pumped was maximized based on the proposed strategy.

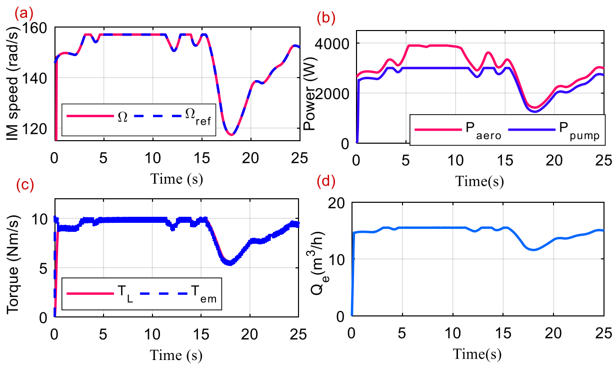

Fig. 9. a) IM mechanical speed, b) WT and pump powers, c) Electromagnetic and load torque, c) Pump flow rate

The stator current signal presents a sinusoidal variation as shown in Fig. 10 (a); Figure 10 (b) shows the varying-time curve of the stator flux which stays constant and equal to 0.8 Wb (the value of the stator flux reference). Figure 10 (c) shows the stator flux vector trajectory. It takes a circular behaviour with radius of 0.8 Wb.

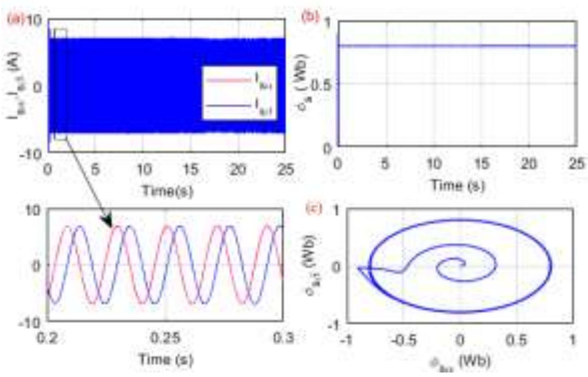

Fig. 10. a) IM stator current, b) Stator flux magnitude, c) Trajectory of the stator flux

6. Conclusion

In this paper, an isolated variable wind turbine coupled to a water pumping system was studied. The proposed configuration comprises a centrifugal pump directly coupled to an induction machine. Evaluated and analyzed for different stages of energy conversion of WT process, the moto pump system is than optimized by the need of an analytic equation related the mechanical speed reference to the wind speed extracted by the WT, the pump system is than optimized by forcing its received power from the WT power in order to optimize the pumped water flow level. The main contribution of this paper consists of maximizing the efficiency of induction motor for every operating point. Besides, with the use of a DTC-SVM the maximization of power was guaranteed. The effectiveness of this proposed strategy is proved by simulation results.

References

[1] Gopal C, Mohanraj M, Chandramohan P, Chandrasekar P. Renewable energy source water pumping systems—A literature review. Renewable and Sustainable Energy Reviews. 25, pp.351-370; 2013.

[2] Sontake VC, Kalamkar VR. Solar photovoltaic water pumping system-A comprehensive review. Renewable and Sustainable Energy Reviews, 59,pp.1038-1067,2016.

[3] Mahela OP, Shaik AG. Comprehensive overview of grid interfaced wind energy generation systems. Renewable and Sustainable Energy Reviews, 57, pp.260-28, 2016.

[4] Vick BD, Neal BA. Analysis of off-grid hybrid wind turbine/solar PV water pumping systems. Solar Energy, 86(5), pp.1197-1207,2012.

[5] Castronuovo ED, Lopes JP. On the optimization of the daily operation of a wind-hydro power plant. IEEE Transactions on Power Systems. 19(3):pp.1599-606,2004;.

[6] Ouchbel T, Zouggar S, Elhafyani ML, Seddik M, Oukili M, Aziz A, Kadda FZ. Power maximization of an asynchronous wind turbine with a variable speed feeding a centrifugal pump. Energy Conversion and Management. , 78, pp.976-984,2014.

[7] Masmoudi A, Abdelkafi A, Krichen L. Electric power generation based on variable speed wind turbine under load disturbance. Energy; 36(8):pp5016-26,2011.

[8] Kallel R, Boukettaya G, Krichen L. Control management strategy of stand-alone hybrid power micro-system using super-capacitor. International Journal of Renewable Energy Research (IJRER),4(1):210-23. 2014.

[9] Slootweg JG, De Haan SW, Polinder H, Kling WL. General model for representing variable speed wind turbines in power system dynamics simulations. IEEE Transactions on power systems, 18(1):pp144-51, 2003.

[10] Hajian M, Markadeh GA, Soltani J, Hoseinnia S. Energy optimized sliding-mode control of sensorless induction motor drives. Energy Conversion and Management. ; 50(9):pp.2296-306, 2009.

[11] Amelio M, Bova S. Exploitation of moderate wind resources by autonomous wind electric pumping systems. Renewable energy; 21(2):pp.255-69, 2000.

[12] López-Luque R, Reca J, Martínez J. Optimal design of a standalone direct pumping photovoltaic system for deficit irrigation of olive orchards. Applied Energy. 149, pp.13-23.2015.

[13] Bouzeria, H., Fetha, C., Bahi, T., Lekhchine, S., & Rachedi, L. Speed Control of Photovoltaic Pumping System. International Journal Of Renewable Energy Research, 4(3), 705-713,2014.

[14] Alsofyani IM, Idris NR. A review on sensorless techniques for sustainable reliablity and efficient variable frequency drives of induction motors. Renewable and Sustainable Energy Reviews, 24, pp.111-121. 2013.

[15] Salem, F. B., Derbel, N, Position Control Performance Improvement of DTC-SVM for an Induction Motor: Application to Photovoltaic Panel Position. International Journal of Renewable Energy Research (IJRER), 4(4), 879-892,2014.